PRELIMINARY STABILITY MAPS CREATED USING CATHENA FOR HEATED CHANNELS WITH SUPERCRITICAL FLUIDS

K. Heckman and D.R. Novog
McMaster University, Hamilton, Ontario, Canada

Abstract

Although supercritical water does not undergo a phase change, there are large property variations near the pseudo-critical point which can introduce instabilities at low mass flows or high power levels. Stability maps have been created using CATHENA MOD 3-5d/Rev3 which identify the power to mass flow ratio at which a flow instability is expected to occur for a given inlet enthalpy, inlet throttling, and outlet throttling. The maps exhibit a similar characteristic shape to boiling water stability maps as well as to supercritical water maps created using other modeling tools. They indicate that, as in boiling water flow, there are two regions of instability: an excursive instability region and an oscillatory instability region.

1. Introduction

A supercritical fluid is a fluid at a temperature above the critical temperature, and at a pressure above the critical pressure. For water, this critical point is at 647.1 K and 22.064 Mpa. Supercritical water is of increased interest because of its intended use as the coolant and working fluid in the Supercritical Water Reactor, one of the Generation IV reactor designs in which Canada is taking a lead role.

Nomenclature

C_p	specific heat at a constant pressure	[kJ/kg K]
g	gravitational acceleration	[m/s$^{3]}$
h	enthalpy	[kJ/kg]
K	throttling resistance	[]
N_{SPC}	sub-pseudocritical number	[]
N_{TPC}	trans-pseudocritical number	[]
P	pressure	[MPa]
$\dot{Q}$	heat added	[W/s]
β	volumetric thermal expansivity	[1/K]
ω	mass flow	[kg/s]

<u>subscripts</u>

$_{ext}$	external
$_{in}$	property at the pipe inlet
$_{int}$	internal
$_{pc}$	property at the pseudo-critical point
$_{out}$	property at the pipe outlet

1.1 Supercritical Water Background

Although fluids above the critical pressure do not go through a phase change, there is a significant gradient in the properties near the point referred to as the pseudo-critical point. The pseudo-critical point occurs at the peak in the specific heat for a given pressure, as illustrated in Figure 1. Figure 1 also illustrates the density profile for various pressures at temperatures around the pseudo-critical points. Although not as abrupt, this density change is not unlike the density change experienced as water boils. For this reason, it is expected that the stability concerns exhibited in boiling water flow may also be a concern in supercritical water flow in a heated channel. The following paper outlines the procedure used to develop stability maps using CATHENA MOD3-5d/Rev3 [1] for water in a simple pipe at supercritical conditions.

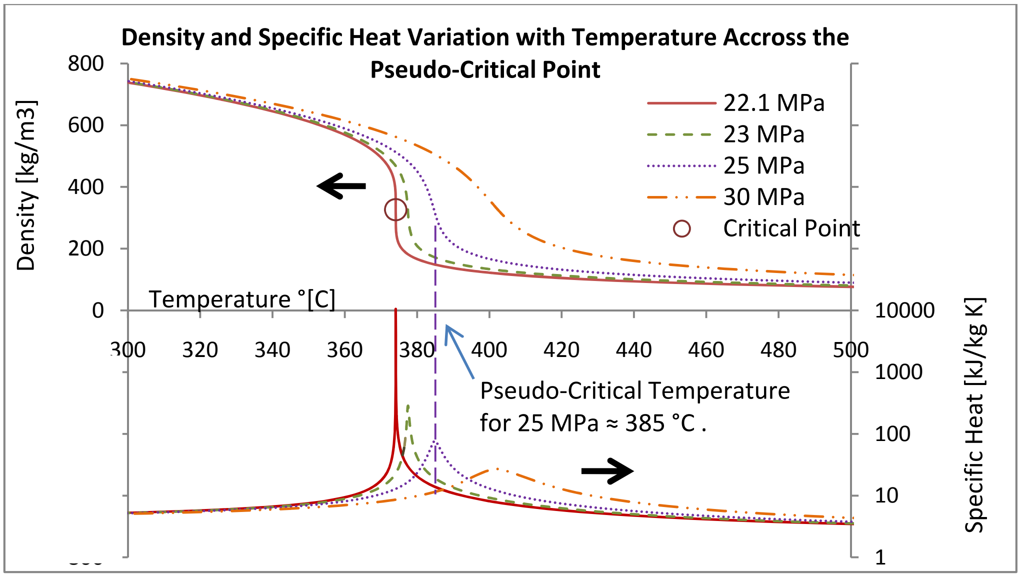

Figure 1: Water property gradients entering the supercritical region

1.2 Subcritical Instabilities

The stability of subcritical, two-phase flow has been studied extensively [2 – 7] and many different types of flow instabilities are defined in boiling water channels. This paper examines a single channel, avoiding instabilities related to multiple channels. Also, since supercritical water is a single phase fluid, instability related to flow regimes and nucleation sites such as flow pattern transition instabilities and geysering, chugging or bumping are not expected. Finally, in this study the heat is added directly to the fluid, avoiding the effect of wall temperature and variations in the heat transfer coefficient that could also compound any instabilities. Other compounding effects of neutron feedback effects such as from the density reactivity coefficient are ignored.

The two types of instabilities most frequently encountered in boiling water channels remain: a density wave oscillation occurring normally at low inlet sub-cooling, and a Ledinegg type flow excursion at higher inlet sub-cooling. The same forms of instability are expected in supercritical fluid flow in a heated channel. The conditions under which these forms of instabilities are expected to occur are presented in the stability map for a vertical channel with upward flow shown in Figure 2, which were created using a linearized model [8]. N_{SPC}, the non-dimensional pseudo sub-cooling of the inlet on the vertical axis, and N_{TPC}, the non-dimensional power to mass flow ratio on the horizontal axis, are defined in Section 2.1.

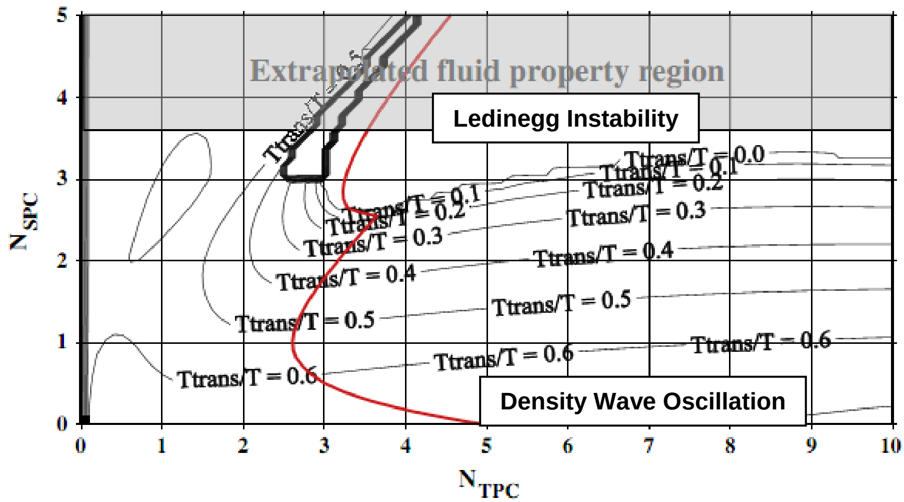

Figure 2: Reference stability map for the case of vertical channel with K_{in}=K_{out}=20 (48 Nodes) created from a linearized analysis. Source: [8]

Ledinegg instabilities are a form of static instability in that they can be predicted based solely on the steady state thermal-hydraulic equations. They occur when the change of internal pressure with changing mass flow is less that the change of external pressure with changing mass flow, $\left.\frac{\delta P}{\delta \omega}\right|_{int} > \left.\frac{\delta P}{\delta \omega}\right|_{ext}$. They are characterized by a sudden change in the mass flow to a lower mass flow at a new steady state [2].

A density wave oscillation is a dynamic instability that is triggered by the large difference in density between the liquid and vapour phases in two-phase flow, or in the case of supercritical water, across the pseudo-critical point. Generally, the density wave oscillation is the result of multiple feedback effects between the propagation of mass flow, density, enthalpy, and pressure drop. It is characterized by a low frequency oscillation of relatively large oscillations. As shown in Figure 2, the relationship between the transit time and the period has been shown to be dependent on the conditions in the channel, varying significantly with the inlet sub-cooling (or pseudo sub-cooling in the case of supercritical water) [8]. Where this ratio approaches zero on the map, the region of excursive instabilities begins.

2. The IAEA benchmark exercise on supercritical water flow stability in a heated channel

With the increased interest in the supercritical water reactor there has been increased focus on the stability of supercritical water. Some linear and non-linear analyses are presented in [9 – 13]. Theoretical analyses and computational models indicate similar stability maps for supercritical water flow as those for boiling water flow, as shown in the reference stability map in Figure 2. An international benchmark exercise was created with the purpose of both verifying the stability maps and establishing the ability of a variety of thermal-hydraulic system codes to model supercritical water flow [14]. Figure 3 presents the geometry for the benchmark exercise.

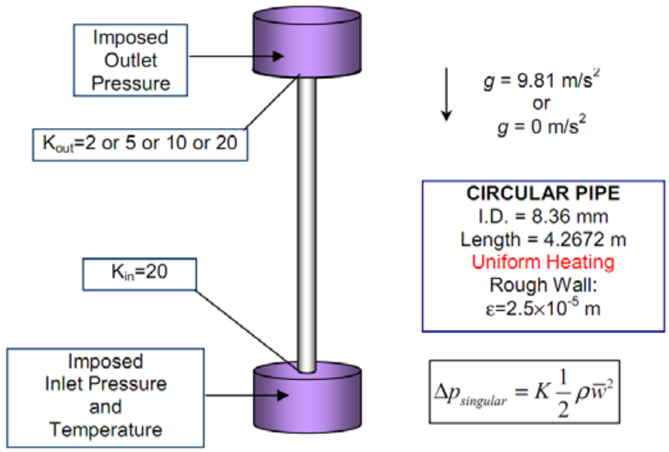

Figure 3: System Specifications for the IAEA Benchmark, Source: [14]

2.1 Non-Dimensional Representation

The stability maps reported for this benchmark exercise were developed in non-dimensional form, similar to the map represented in Figure 2. Ambrosini [10] defined two non-dimensional numbers for characterizing the conditions for flow stability. The sub-pseudocritical number N_{SPC}, shown in Equation (1), represents the pseudo inlet sub-cooling as a measure of the proximity of the enthalpy at the inlet of the pipe to the pseudo-critical enthalpy at a specific pressure. The trans-pseudocritical number, N_{TPC} ,shown in Equation (2) represents the power to mass flow ratio at a specific pressure. [10]

$$N_{SPC} = \frac{\beta_{pc}}{C_{p,pc}}\left(h_{pc} - h_{in}\right) \quad (1)$$

$$N_{TPC} = \frac{\dot{Q}}{\omega_{in}}\frac{\beta_{pc}}{C_{p,pc}} \quad (2)$$

The stability threshold for a given sub-pseudocritical number, N_{SPC}, is defined as the value of trans-pseudocritical number, N_{TPC}, at which an oscillation or excursion develops .

3. CATHENA Model

Multiple runs of the input model illustrated in Figure 4 were used to determine the stability thresholds that make up the stability map. The input model consisted of a simple pipe of anywhere from 20 to 80 nodes between two reservoirs of constant pressure. Heat was added uniformly and directly to the fluid in the pipe through the application of a heat input boundary condition. This eliminated any delay and dampening that may have come from the heat transfer between the pipe wall and the heat source. Junction resistance system models were used both at the inlet and the outlet of the pipe to model inlet and outlet throttling.

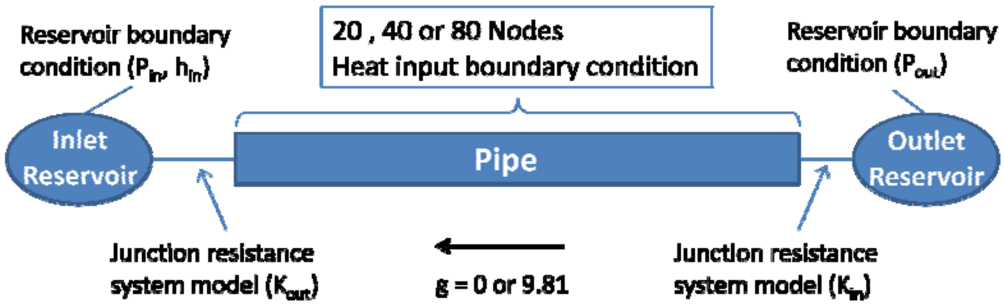

Figure 4: CATHENA Input Model

A run consisted of first determining the appropriate pressure drop across the two reservoirs that would have the instability occur between 0.04 kg/s and 0.08 kg/s. A steady state was established with no heat addition to the fluid. The mass flow at this point would usually be between 0.08 kg/s and 0.10 kg/s. A control model within CATHENA was used to add heat directly to the fluid, which would force the mass flow to decrease. The heat was added in two stages: a quick power ramp stage in order to progress to the expected region of the instability, followed by a very slow power ramp so as to avoid any secondary heat addition effects. The code was allowed to continue unperturbed with the assumption that numeric truncation errors would be enough to trigger an instability (no forcing functions were used to initiate the instability). Runs were repeated for varying sub-pseudocritical number, outlet throttling resistances, inlet throttling resistances, nodalization and orientations of the heated channel (vertical upward and horizontal). The transients were automatically terminated on a large divergence of the trans-pseudocritical number.

Control models were introduced which would calculate the trans-pseudocritical number according to Equation (2), and automatically detect the unstable variation of this number. The automated instability detection would flag an oscillatory instability on a decrease in the trans-pseudocritical number (time-averaged in order to omit high frequency variations) followed by an oscillation within an adjustable maximum period. The excursive instabilities were more difficult to define. The automated instability detection would flag an excursive instability when the rate of change of the trans-pseudocritical number was above 0.1. Both of these detection methods are dependent on the rate of heat input, the magnitude of the oscillations and the input conditions of the heated channel.

An example of a run ($N_{SPC} = 1.0, K_{out} = 20$) which terminated in an oscillatory instability is shown in Figure 5. This same transient is represented in non-dimensional form in Figure 6. Also illustrated in Figure 6, increasing the sub-pseudocritical number to 3.0, the instability is delayed and when it does occur is excursive. The dashed blue lines in Figure 6 represent the instability detection control model activating based on perturbation of N_{TPC}. The threshold detection control model is reset if this perturbation does not develop into an instability. The stability threshold for each run is identified on the transient.

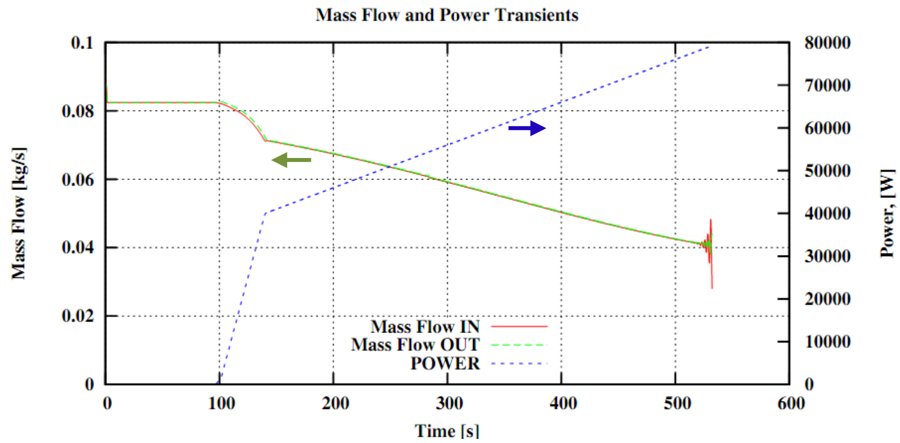

Figure 5: Mass flow and power transient for vertical flow; $N_{SPC} = 1.0$, 40 nodes, $K_{in} = K_{out} = 20$

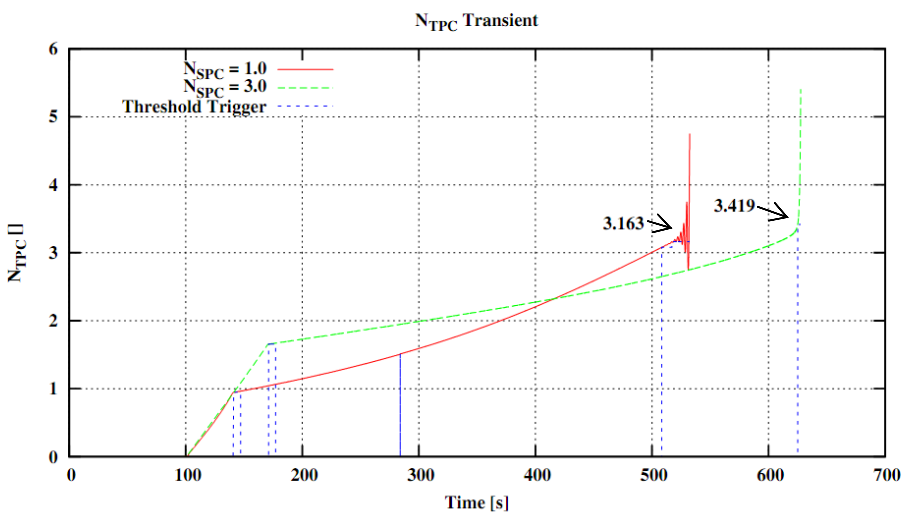

Figure 6: N_{TPC} transient for vertical flow in a simple pipe with increasing uniform heating; $N_{SPC} = 1.0$ and 3.0, 40 nodes, $K_{out} = K_{in} = 20$

4. Preliminary Stability Maps

A variety of runs for different sub-pseudocritical numbers and different outlet throttling resistance were assembled to create the stability maps for supercritical water flow in a heated channel, an example of which is shown in Figure 7. The encircled data points indicate instabilities of an excursive nature, where-as non-circled points indicate an oscillatory instability. An excursive instability region is evident in the high sub-pseudocritical cases with high outlet throttling. The destabilizing effect of the outlet throttling, particularly for the flow excursions, is also clear as there is a large decrease in the stability threshold with increasing outlet throttling resistance. The opposite stabilizing effect of inlet throttling is shown in Figure 8. The transit time to oscillation period ratios for the data in Figure 7 are presented in

TRANSIT TIME to OSCILLATION PERIOD RATIOS

K_{out}				
20	10	5	2	0

N_{TPC}	**3**	--	--	--	0.30	0.32
	2.5	--	--	0.33	0.36	0.38
	2	0.65	0.36	0.40	0.43	0.45
	1.5	0.42	0.45	0.48	0.50	0.52
	1	0.52	0.54	0.56	0.58	0.31
	0.5	0.63	0.64	0.66	0.69	0.73
	0	0.74	0.76	0.80	0.84	--

Table 1 in which ratios coincide roughly with the contour plot shown in the referenced stability map in Figure 2.The discrepancy with the value for the case with $N_{SPC} = 2$ and $K_{out} = 20$ is due to the difficulty in distinguishing between excursive and oscillatory instability for this case.

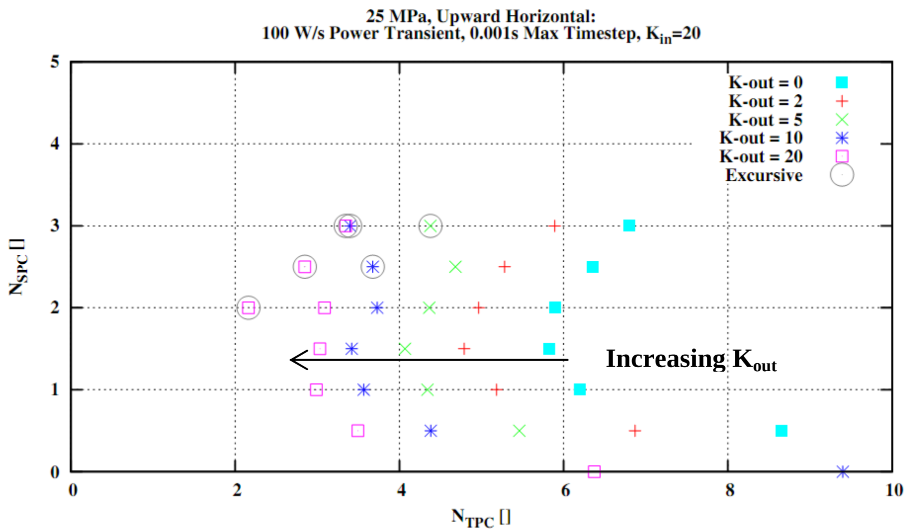

Figure 7: Preliminary stability map for horizontal flow in a heated channel, 40 nodes at 25 MPa System Pressure (maximum time-step = 0.001s, K_{in} = 20)

TRANSIT TIME to OSCILLATION PERIOD RATIOS

		K_{out}				
		20	**10**	**5**	**2**	**0**
N_{TPC}	**3**	--	--	--	0.30	0.32
	2.5	--	--	0.33	0.36	0.38
	2	0.65	0.36	0.40	0.43	0.45
	1.5	0.42	0.45	0.48	0.50	0.52
	1	0.52	0.54	0.56	0.58	0.31
	0.5	0.63	0.64	0.66	0.69	0.73
	0	0.74	0.76	0.80	0.84	--

Table 1: Transit time to Period Ratio for data presented in Figure 7 Figure 7

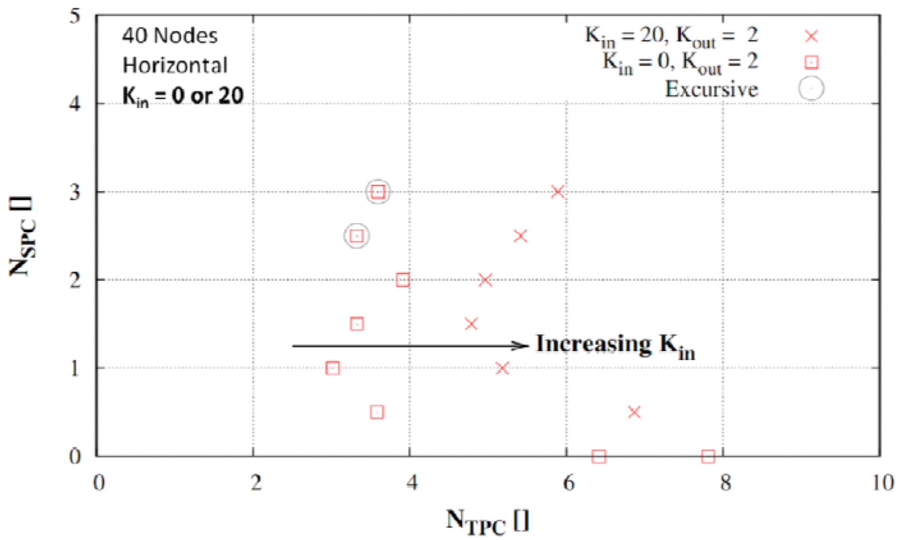

Figure 8: Stability map dependence on inlet throttling

4.1 Nodalization effects

The case with a sub-pseudocritical number of 1.0, an inlet throttling resistance of 20, and an outlet throttling resistance of 10 was selected as a base case to determine the appropriate nodalization and time-steps for all of the transient simulations. A maximum time step of 0.01s was required in order to detect the instabilities for the base case. Preliminary studies considering channel nodalization between 15 and 50 nodes, and the time-steps between 0.01s and 0.0001s suggested that a maximum time-step of 0.001s is appropriate for any nodalization, and that 40 nodes should be sufficient. As an alternative, to allow for more variation in the time-step between the different cases with different maximum velocities and when conducting nodalization studies, a control model was added which would use the calculated courant number to dynamically adjust the time-step. Mimicking the time-step control of explicit system codes, the control model would adjust to time-step at each successive time-step such that the courant number would remain constant. The preliminary stability maps were initially created with 40 Nodes and a maximum time-step of 0.001s. Extended time-step studies were conducted on the stability map, as shown in Figure 9 and support the time-step chosen. However, further nodalization studies on the entire map, shown in Figure 10Figure 10, suggest that the nodalization may need to be more refined to achieve convergence in the results.

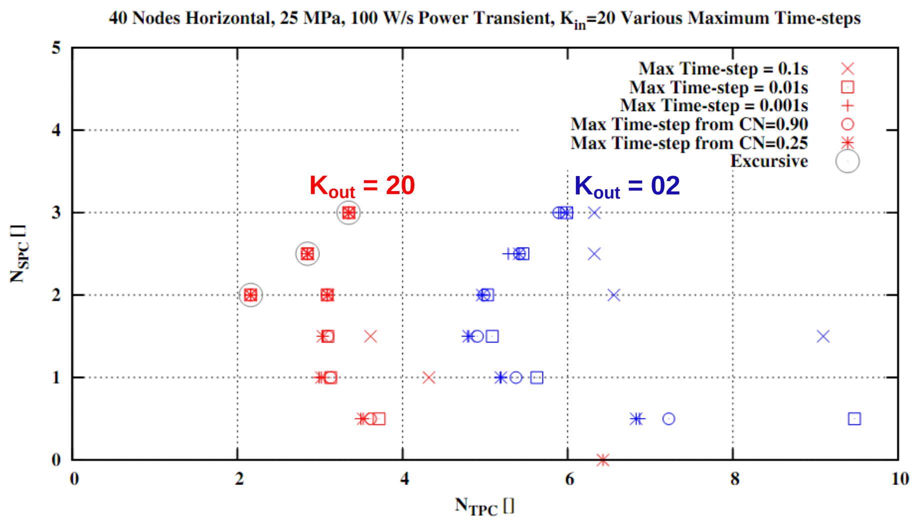

Figure 9: Stability Maps for Horizontal channel with various maximum time-steps

The nodalization discrepancies at the low pseudo-subcooling values and low outlet throttling resistances, possibly due to the higher fluid velocities that are encountered under these system conditions, and are consistent with other similar studies [8] and with the time-step studies presented above. The discrepancies in the excursive instabilities at higher pseudo-subcooling, and were not expected. Figures Figure 11 - Figure 13 illustrate the transients of trans-pseudocritical number for various cases with higher pseudo-subcooling where the stability threshold obtained using 80 nodes is significantly different from the stability threshold using 40 nodes. Figure 11 and Figure 12**Error! Reference source not found.** show distinct excursions for the transients run with 80 nodes, whereas with 40 nodes, the excursion appears diffused, although still present, which then develops into an oscillatory instability. The transients in Figure 12also demonstrate a mixed-excursive/oscillatory behaviour for which the stability threshold is difficult to define. It is likely that the conditions for these runs put the system on the horizontal section of the reference stability map presented in Figure 2, which also corresponds to the boundary between excursive and oscillatory instabilities.

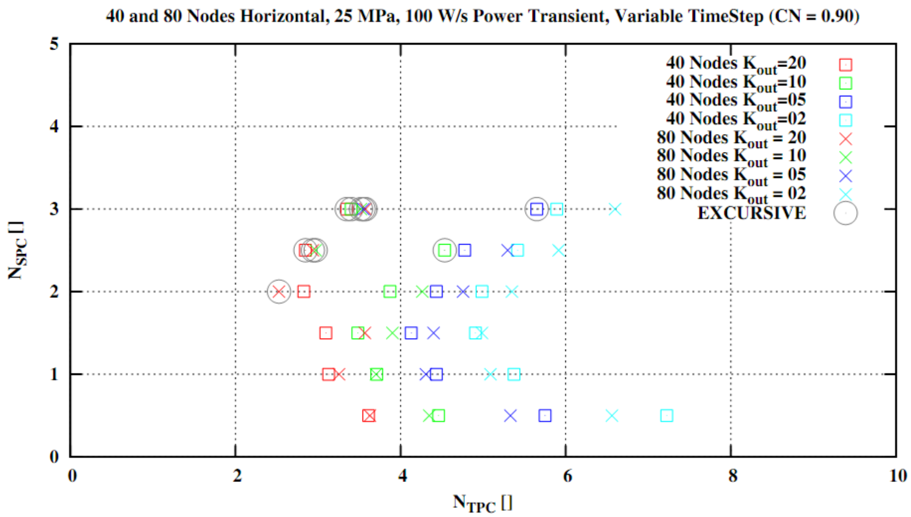

Figure 10: Stability map dependence on nodalization for horizontal flow

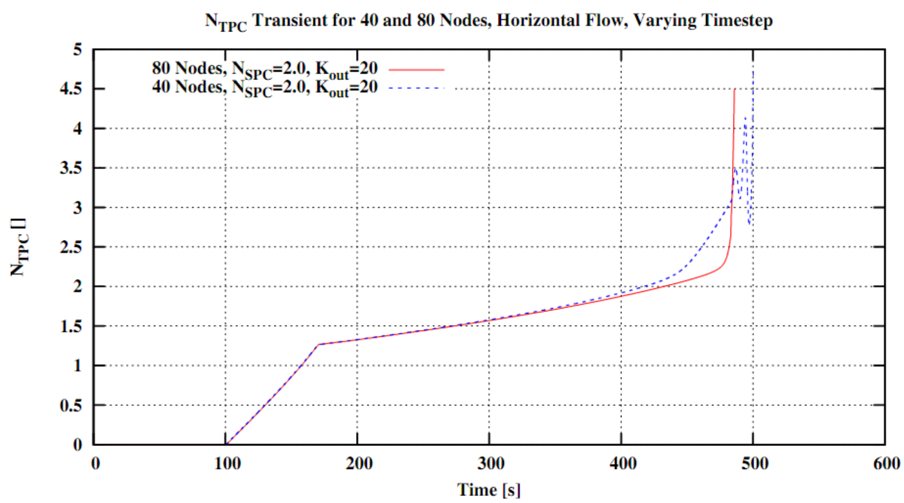

Figure 11: Horizontal flow transients for different nodalization of the heated channel (40 and 80 Nodes, Courant Number =0.9, $N_{SPC} = 2.0$, $K_{out} = K_{in} = 20$)

Figure 13, illustrates a transient that terminates in an oscillatory instability for both 40 and 80 nodes, but the instability occurs at a higher threshold when run with 80 nodes. There appears to be a sudden change in the trans-pseudocritical number which then leads to a higher threshold value of the trans-pseudocritical number. Since the magnitude of this sudden change in trans-pseudocritical number increases with increasing pseudo-subcooling and increasing outlet resistance, it may be a demonstration of a very minor excursion, or could simply be a manifestation of the supercritical water properties used in CATHENA. Further examination into the conditions under which these small changes in the trans-pseudocritical number occur is required.

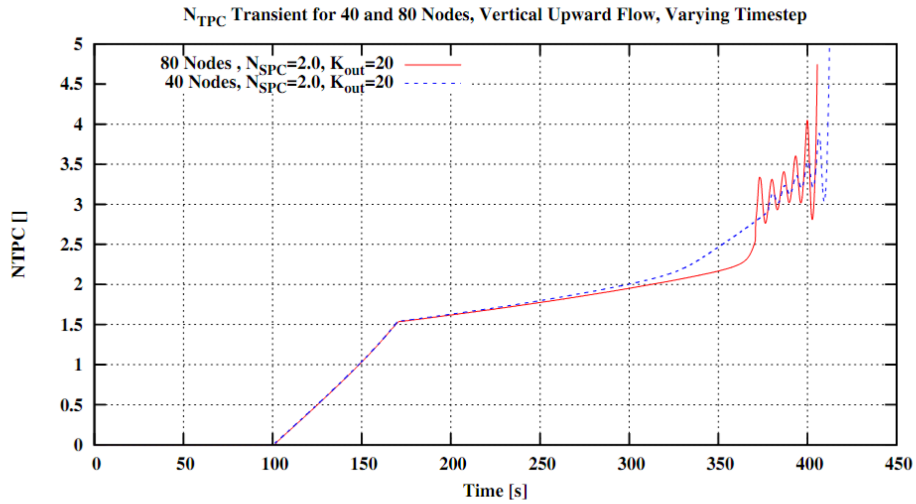

Figure 12: Horizontal flow transients for different nodalization of the heated channel (40 and 80 Nodes, Courant Number =0.9, $N_{SPC} = 3.0$, $K_{out} = K_{in} = 20$)

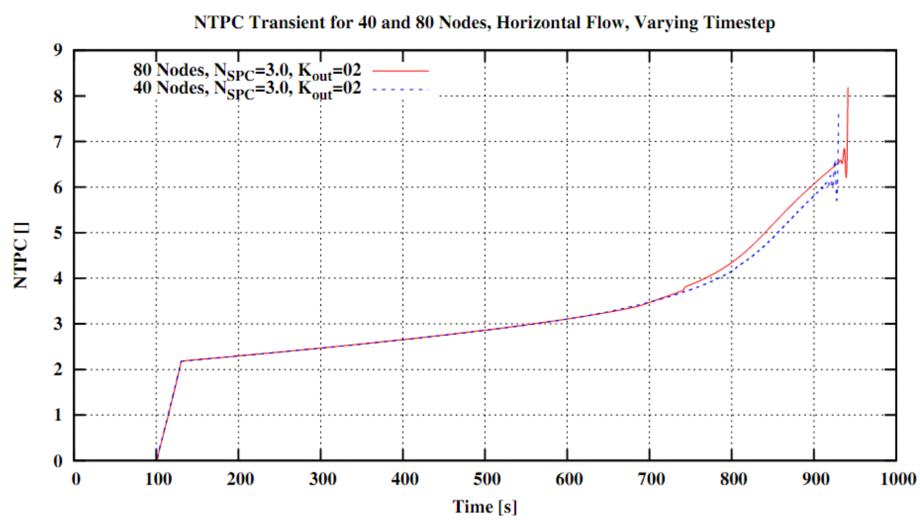

Figure 13: Horizontal flow transients for different nodalization of the heated channel (40 and 80 Nodes, Courant Number =0.9, $N_{SPC} = 3.0$, $K_{out} = K_{in} = 02$)

4.2 Flow orientation

As shown in Figure 14, comparing the horizontal to upward vertical stability maps, both created with 80 nodes, produces good agreement except in the boundary between excursive and oscillatory instability. This conformity is consistent with similar stability map analyses [8] but is not produced with the maps created using 40 nodes. Figure 15 shows the transients for runs with all conditions similar except for flow orientation at high pseudo-subcooling. It is evident that the effect of gravity reduces the magnitude of the excursion. It appears as though a flow excursion takes place at the same conditions as in the horizontal flow, but that the system is able to recover at a new stable mass flow rate. After this excursion, the system continues until an oscillatory instability is recorded. It is only the second threshold that is identified on the stability map in Figure 14, but both thresholds exist in the vertical orientation. It is postulated that under certain conditions, such as those shown in Figure 15, there are two-loci of instability separated by a region of stability. Hence during some transients and configurations it is possible that upon reaching the first instability, conditions change in a direction which allows a new stable flow to be obtained (as expected in a Ledinegg excursion). This stable flow is maintained until the second instability is initiated.

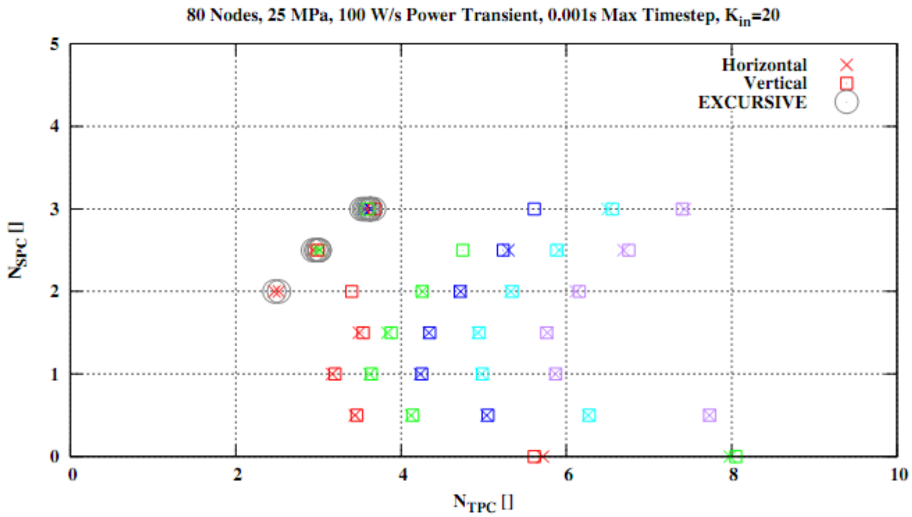

Figure 14: Comparing Horizontal to Vertical Upward flow stability thresholds for 80 Nodes

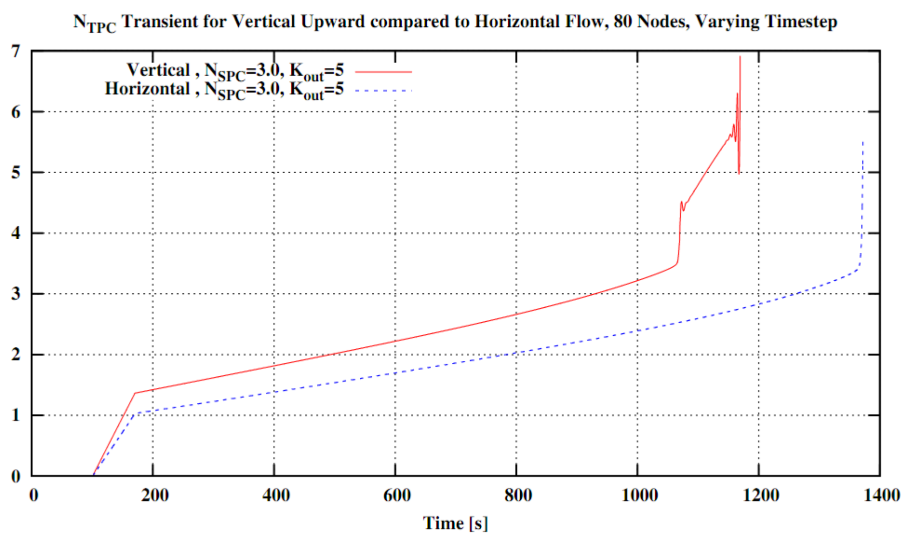

Figure 15: Vertical Upward flow and Horizontal flow transients
(80 Nodes, $N_{SPC} = 3.0$, $K_{out} = 5$)

4.3 Comparison of CATHENA results to other models

In

Figure 16, the stability maps created using CATHENA (with 80 Nodes) are compared to those created with a reference stability map produced with a linearized stability model for the same heated channel [8]. The stability maps determined using CATHENA illustrate the same general shape, but the thresholds are shifted to higher trans-pseudocritical values for all cases. It appears that the threshold map determined for each outlet throttling are consistent when the resistance value is halved, however, whatever difference there is in the application of the outlet throttling resistance would also present itself in the inlet throttling application, so such a straight forward accounting for the discrepancies is not likely. Other factors that could contribute to the discrepancies are the model used to determine the friction factor, the power ramp applied if not sufficiently low to inhibit addition stability effects, and most notably the method of selection of the stability threshold. A visual selection of the threshold was used to create the referenced stability map [8]. The automated threshold detection method reported in this paper shows a weakness particularly in determining the threshold value for instabilities near the transition from an oscillatory to an excursive form, as well as a susceptibility to the natural rate of change of the trans-pseudocritical number. For comparison, the threshold values for the cases with 40 nodes were selected visually with no influence from the automated detection. The maps thus created and presented in

Figure 17 show much better agreement with the referenced stability map, though still shifted by half the outlet throttling. The transients run using CATHENA also show an excursive region occurring at lower subcooling values than those reported in similar super-critical water stability analyses.

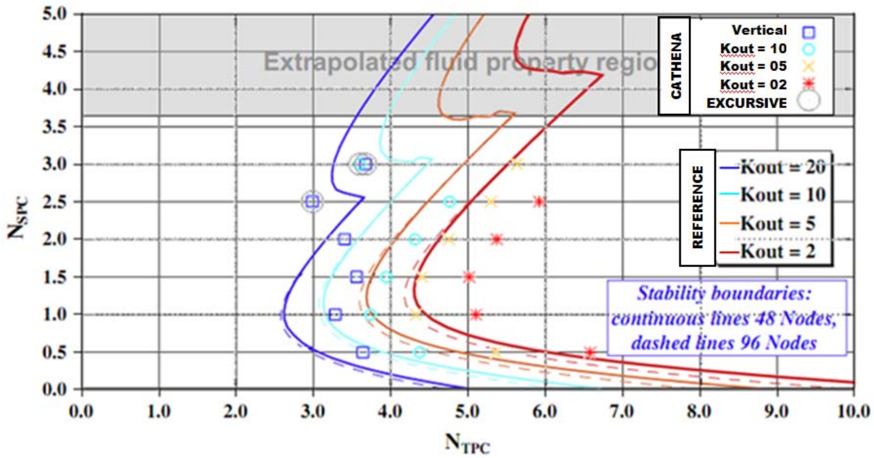

Figure 16: Vertical Stability Map Comparison (K_{out} = 2, 5, 10 and 20) 80 Nodes, Max Time-step controlled with Courant Number = 0.90

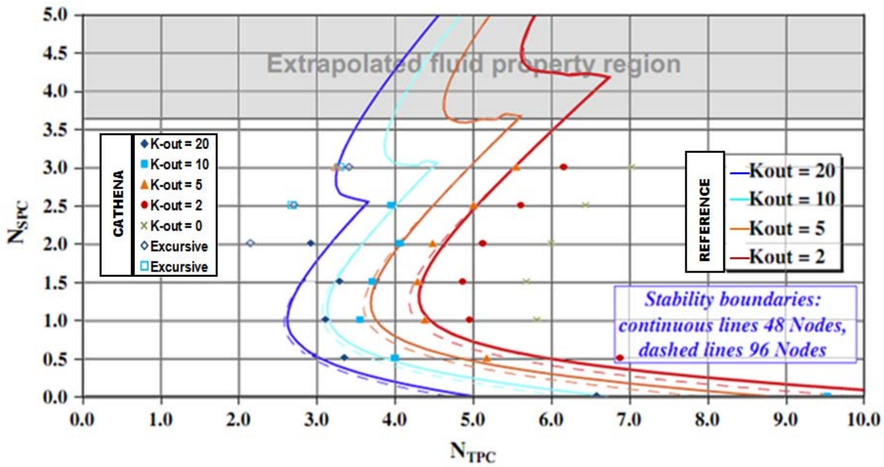

Figure 17: Vertical Stability Map Comparison (K_{out} = 2, 5, 10 and 20) 40 Nodes, visual inspection

5. Conclusion

The stability maps for supercritical water in a heated channel created using CATHENA are similar both to the established maps for boiling water and to similarly created maps for supercritical water flow. The excursive instabilities occur at much lower sub-pseudocritical number than the region previously established for the same system specifications. The stability thresholds determined using CATHENA are also uniformly higher, indicating a higher heat input or lower mass flow permissible for given inlet conditions and outlet throttling. The stabilizing effect of inlet throttling and de-stabilizing effect of outlet throttling was reproduced as expected. The period of the oscillatory instabilities is on the order of the channel transit time and varies with system conditions in accordance with the attributes of a density wave oscillation. The dampening effect of nodalization, particularly on the excursive instabilities, and the appropriate level of nodalization need further investigation. Future work also includes investigation into the sudden changes in the trans-pseudocritical number at high nodalization, and the underlying phenomena, as well as extension to the channel dimensions, conditions, and power levels expected in the CANDU SCWR.

6. Acknowledgements

The guidance and suggestions from Bruce Hanna and Thomas Beuthe from Atomic Energy of Canada Limited are gratefully acknowledged.

7. References

[1] Hanna, B.N., “CATHENA: A thermalhydraulic code for CANDU analysis”, Nuclear Engineering and Design, 1998, pp113-131.

[2] Boure, J.A., Bergles, A.E. and Tong, L.S. “Review of two-phase flow instability”, Nuclear Engineering and Design, 1973, , pp. 165-192.

[3] Belblidia, L.A. and Bratianu, C. “Density-Wave Oscillations”, Annals of Nuclear Energy, 1979, pp. 425-444.

[4] Fukuda, K. and Kobori, T. “Classification of two-phase flow instability by density wave oscillation model”, Journal of Nuclear Science and Technology, 1979, pp. 95-108.

[5] Ambrosini, W., Di Marco, P. and Ferreri, J.C. “Linear and nonlinear analysis of density wave isntability phenomena”, International Journal of Heat Technology, 2000, pp. 27-36.

[6] D'Auria, F. et al. “State of the Art Report on Boiling Water Reactor Stability, Committee on the Safety of Nuclear Installations”, OECD Nuclear Energy Agency, 1997, OCDE/GD(97)13.

[7] Walter, H. “Density wave oscillation in the horizontal parallel tube paths of the evaporator of a natural circulation heat recovery steam generator - a theoretical investigation”, WSEAS Transactions on Heat and Mass Transfer, 2007, pp. 17-27.

[8] Ambrosini, W., “Assessment of Flow Stability in a heated channel with different fluids at supercritical pressures”, Annals of Nuclear Energy, 2010,

[9] Ambrosini, W. “On the analogies in the dynamic behaviour of heated channels with boiling and supercritical fluids”, Nuclear Engineering and Design, 2007. pp. 1164-1174.

[10] Ambrosini, W. and Sharabi, M. “Dimensionless parameters in stability analysis of heated channels with fluids at supercritical pressures”, Nuclear Engineering and Design, 2008, pp. 1917-1929.

[11] Ambrosini, W. “Lesson learned from the adoption of numerical techniques in the analysis of nuclear reactor thermal-hydraulic phenomena”, Progress in Nuclear Energy, 2008, Vol. 50.

[12] Ortega Gomez, T., et al., “Stability analysis of a uniformly heated channel with supercritical water”, Nuclear Engineering and Design, 2008, pp. 1930-1939.

[13] Ambrosini, W., “Specifications for a benchmark exercise on flow stability in heated channels with supercritical fluids”, Pisa, Italy : University of Pisa, 2009. Report DIMNP RL 1214(2009) Rev. 2.